

https://doi.org/10.1070/QEL16884

New type of large-scale experiments for laboratory astrophysics with collimated jets of laser plasma in a transverse magnetic field

Yu.P. Zakharov, A.G. Ponomarenko, V.A. Terekhin,
V.G. Posukh, I.F. Shaikhislamov, A.A. Chibranov

Abstract. **We report the results for the first complex experiment on the formation of an extended (up to ~0.5 m) plasma jet in a magnetic field (up to 300 G) in vacuum. The jet appears due to the injection of laser plasma bunches with a kinetic energy up to ~50 J across the magnetic field (in a solid angle $\Omega \approx 1$ sr) and a high degree of magnetisation of ions on the calculated scale field-induced deceleration of the bunch as a part of a sphere. A plastic target (polyethylene) has been irradiated by a CO_2 laser in the most energy-efficient regime (near the plasma formation threshold), implemented at the expense of a wide radiation spot (diameter 2–3 cm) on the target. In a new-type model Super-Jet experiment on a large KI-1 facility at the Institute of Laser Physics, Siberian Branch, Russian Academy of Sciences (ILP SB RAS), the probe data on the internal structure and dynamics of plasma concentration and magnetic field strength in transverse jets, on the influence of instabilities and Hall effect have been obtained for the first time in laboratory modelling of space and astrophysical jets.**

Keywords: *plasma jets, transverse magnetic field, laser plasma, Larmor radius of ions, diamagnetic cavity, Hall effect, laboratory astrophysics.*

1. Introduction

From the very beginning of extensive research on the production of a laser plasma (LP) during irradiation of various targets, great attention has always been attracted by the possibility of the formation of various types of LP jets both due to purely classical hydrodynamic effects [1] and the generation of spontaneous magnetic fields exceeding 1 MG [2]. Both in earlier studies [3–6], and particularly in recent years [7–16], experiments on the influence of external, quasi-stationary and superstrong (up to 10 MG and more) magnetic fields $\boldsymbol{B}_0$ on the dynamics of the LP expansion are of the greatest interest. This is because in these experiments the formation of jets propagating along [11–15] or across [3–10] the field $\boldsymbol{B}_0$ over considerable distances is almost always observed. Currently, such jets are of particular interest in relation to the attempts [11–14] of conducting experiments with LP (or with a plasma focus [15]) in strong magnetic fields to simulate the propagation of astrophysical (or magnetospheric [6, 7]) jets. However, so far in modelling the propagation of jets in magnetic fields, only the first results have been obtained, despite significant advances [11] in solving the more complex problem of studying the instabilities of these jets in a magnetised background medium.

To a large extent, this may be due to some common features in conducting vacuum experiments, in which the maximum attainable fields (up to $B_0 \approx 30$ kG and higher) with usually moderate plasma energy E_{e0} (not higher than 10 J) were used to ensure the highest degree of ion magnetisation. Under these conditions, the total transverse size of the magnetic flux tube, in which the LP with such energy will propagate, amounts to $2R_b \approx 14$ mm [17], where the characteristic radius of spherical plasma bunch deceleration by the field (according to the Raiser model [18]) is

$$R_b = (3E_{e0}/B_0^2)^{1/3} \approx 7 \text{ mm}. \quad (1)$$

As a result, on such scales, it becomes impossible to use any other diagnostic methods (for example, probe diagnostics), except for optical ones, so that the structure and dynamics of plasma and magnetic fields, as a rule, remain unexplored. Of course, the condition of magnetisation of LP ions with the 'directed' Larmor radius of ions $R_L \propto (m/z)V_0 \approx 2$ mm (for the LP front expansion velocity $V_0 \approx 200$ km s^{-1} and the ion mass-to-charge ratio $m/z \approx 3$ amu) in this case will be satisfied. In other words, the required critical value $\varepsilon_b^* \approx 0.5$ for the ion magnetisation criterion

$$\varepsilon_b = R_L/R_b \approx 0.3 < \varepsilon_b^*, \quad (2)$$

established for the first time in the experiments [19, 20] on the facility KI-1, will surely be achieved (and the LP will be significantly decelerated at a distance equal to the radius R_b).

In this work, we used another method for implementing condition (2) at the expense of a significant increase in the LP effective energy E_{e0} at moderate fields B_0. Earlier this method was successfully used [21] on the KI-1 facility for solving one more fundamental problem of laboratory astrophysics, namely, the bunch generation of collisionless shock waves (CSWs) in a magnetised background plasma. As in Ref. [21], we used here the space-time relations discovered not long ago [22, 23] between the geometry of the LP expansion from a flat target (in the form of a half-ellipsoid with the large semiaxis a directed along the normal $\boldsymbol{n}$ to the target at $t \to \infty$) and the parameters of laser radiation (pulse duration τ, wavelength λ and energy Q, focal spot diameter $D = 2r_0$, intensity I) and

Yu.P. Zakharov, A.G. Ponomarenko, V.G. Posukh, I.F. Shaykhislamov, A.A. Chibranov Institute of Laser Physics, Siberian Branch, Russian Academy of Sciences, prosp. Akad. Lavrent'eva 15B, 630090 Novosibirsk, Russia; e-mail: kilz@mail.ru;
V.A. Terekhin Russian Federal Nuclear Centre 'All-Russian Scientific Research Institute of Experimental Physics', prosp. Mira 37, 607188 Sarov, Nizhny Novgorod region, Russia

Received 24 October 201
Kvantovaya Elektronika **49** (2) 181–186 (2019)
Translated by V.L. Derbov

target (average $\langle m/z\rangle$ of LP ions, initial electron temperature T_{e0} as functions of $I\lambda^2 \propto Q\lambda^2/(\tau D^2)$) [24]).

2. Formulation of experiments on modelling transverse jets on the KI-1 laser facility at the ILP SB RAS. Required similarity criteria

The main similarity criteria for modelling astrophysical jets in a vacuum in the simplest (non-relativistic) formulation are the magnetisation criterion of ions ε_b (2) and the geometrical criterion introduced below $\Lambda = \tau V_0/r_0$ associated with the initial energy of the LP required for this model experiment. Since in simulating jets, as in simulating a CSW [21], the initial stage of the formation of a (quasi-)spherical diamagnetic cavity when LP interacts with a magnetic field [17] may also be important, it is necessary to introduce an appropriate criterion for the formation of the largest cavity for LP in a flat target. This criterion corresponds to the implementation of the regime in which the effective energy E_{e0} is substantially greater than the real kinetic energy of the plasma E_k. As the simplest example, let us consider the expansion of a real spherical LP cloud of radius R as expansion of six separate conical parts-segments (like pyramids with height $H \approx R$ and apex angles $\alpha \times \beta \approx 90° \times 90°$), where four parts are located at the equator of the sphere and two parts are located at the poles. At the LP front, each part will produce a dynamic pressure $p_d \approx n\langle m/z\rangle V_0^2$ normal to its base, where the electron concentration n is determined by the expression

$$n \approx 3N_{e0}/(4\pi R^3). \quad (3)$$

The total effective number of electrons N_{e0} in a spherical cloud (in the case of n homogeneity) also determines the total kinetic energy of such a cloud.

$$E_0 = 0.3N_0\langle m/z\rangle V_0^2. \quad (4)$$

From Eqns (1), (3) and (4) it obviously follows that both the actual spherical LP cloud with real energy E_0 and the number of electrons N_0, and its part (in the considered case $1/K \equiv 1/6$) can produce diamagnetic cavities of the same radius R_b, only if in Eqn (1) the appropriate value of effective energy is used for all the segments. In the considered example it is the energy $E_{e0} = 6E_k$. Here E_k is the energy of one of the segments ($K = 6$) that form a sphere and produce pressures on its base (front), comparable to the pressure p_d (for balance with a close field pressure proportional to $B_0^2/8\pi$).

As a result, using much simpler implementable LP bunches from flat targets (with the energy smaller by K times) rather than spherical ones [20], it is possible to form caverns that are only two times smaller in linear size (one radius R_b). The problem for such directionally (rather than isotropically) expanding LP bunches is how fast and strongly they can expand, ensuring the flow of the diamagnetic current along its entire boundary. Otherwise, they can be polarised and propagate in the regime of electric drift across the magnetic field, without expulsing it at the desired distance R_b (1). Obviously, such parasitic processes will have a stronger influence on the possibility of using the method of effective energy E_{e0}, the smaller are the angles $\alpha \approx \beta$ (of the sectors) that can be implemented for the types of targets and radiation sources used.

Earlier, since 2005, such flat (or slightly convex) caprolon and more promising polyethylene targets with a diameter of $D = 2r_0 \approx 2–2.5$ cm (slightly larger than the diameter of the focusing spot for CO_2 lasers) were successfully used in model experiments in vacuum with magnetic fields of various geometries. Quantitative grounds for this were established in Ref. [21] based on probe measurements and the magnitude of the total angle Ω of the expansion of the LP from such targets. The angle $\Omega \approx 1$ sr ($\alpha \approx \beta \approx 57°$) approximately corresponds to the angles calculated in the framework of the known models of the LP formation (at distances $R \gg r_0$) [22, 23]. These parameters of experiments with LP, which determine its important characteristic, namely, the angle of initial expansion, allow the introduction of the second similarity criterion of the problem $\Lambda = \tau V_0/r_0$, since according to, e.g., Ref. [22], the angle Ω corresponds to ~60° only when $\Lambda \geqslant 0.15$.

Under the conditions of the Super-Jet experiment (Fig. 1), the preliminary results of which were published in Ref. [16], the value of Λ is not smaller than 1 (at t = 0.1 μs, V_0 = 100 km s^{-1}, r_0 = 1 cm). It is certainly sufficient even for the first, at t = 100 ns, radiation peak in the case of the main pulse having microsecond duration. This was confirmed by plasma image recording using an electron-optical converter (EOC) (Fig. 2) and by experimental data (Fig. 3) of measuring the angular distribution $F(\theta)$ of the ion flux density (at maximum) on the probes. Signals from Langmuir probes installed at a distance of R_p from the target are presented in Fig.4. In the leading part of the current pulse (at $t < 8$ μs), which has a characteristic velocity $V_{0f} \approx 120$ km s^{-1} at the end of the leading edge, the potential $|U_p| = 35–55$ V slightly increases the probe currents I_p. Basing on these currents, the concentration n of the LP electrons, $n \approx J_i/[eV_{0f}(1+\gamma)]$ ($J_i = I_p/S_p$, where S_p is the probe area, $\gamma \approx 0.7$ is the secondary ion–electron emission coefficient), as well as the total effective number $N_{e0} \approx 10^{19}$ ($N_{e0} \approx 4\pi R_p^2 \int J_i(t)\mathrm{d}t/e$) [20, 21, 25], can be estimated. The corresponding effective energy of the LP bunch is $E_{e0} \approx 250$ J for the LP front velocity $V_{0f} \approx 120–140$ km s^{-1} and the average ratio $\langle m/z\rangle \approx 2.5$ amu. The estimated size (1) of the region

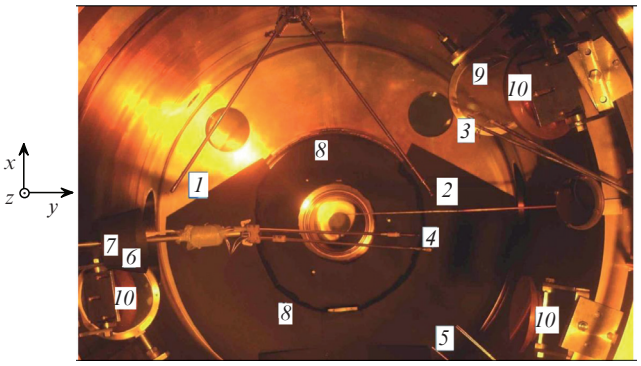

Figure 1. (Colour online) Layout of probes and laser optics in the central plane of the chamber (diameter 120 cm) of the KI-1 facility: (*1*) and (*2*) thin (diameter 20 microns) Langmuir probes IK1 and IK2 of the 'Tsirkul' system (together with its magnetic probes RM1H and RM2H, oriented along the camera z axis, along which the field $\boldsymbol{B}_0$ is directed); (*3*) probe P1; (*4*) probe P0; (*5*) ion collector; (*6*) paper screen near the target (diameter 11.5 cm); (*7*) location of the target (at a distance of 35 cm from the centre of the camera); (*8*) sheets of black paper on the walls of the chamber to reduce the illumination of optical devices by a LP near the target; (*9*) NaCl lenses; (*10*) swivel copper mirrors for two beams, irradiating the target; the coordinates x, y, z are measured from the centre of target (*7*).

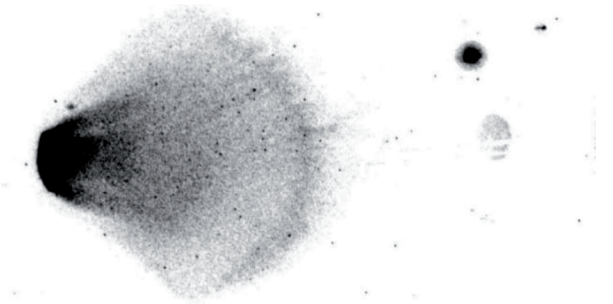

Figure 2. Images obtained using EOC at the time moment $t = 4$ μs (exposure time 140 ns) with the magnetic field $B_0 = 300$ G. The spot edge diameter on the left is 11.5 cm, and hydrogen H_2 (~0.17 mTorr) is injected to increase the brightness of the LP in the chamber of the KI-1 facility, which does not affect the distribution of LP. Small flutes are visible at the leading edge of the expanding LP. The expansion angle is ~80°.

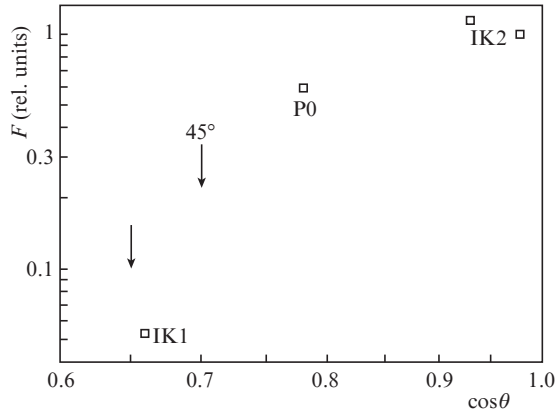

Figure 3. Angular distribution $F(\theta)$ of the normalised LP flux density J_i (with different distances from the probes to the target taken into account), obtained from the maximum signals of the probes, for different angles θ to the target normal. The left arrow indicates the angle approximately corresponding to the position of the edge of the screen *6* in Fig. 1. The angle $\theta \approx 45°$ corresponds to the boundary of the distribution F(θ).

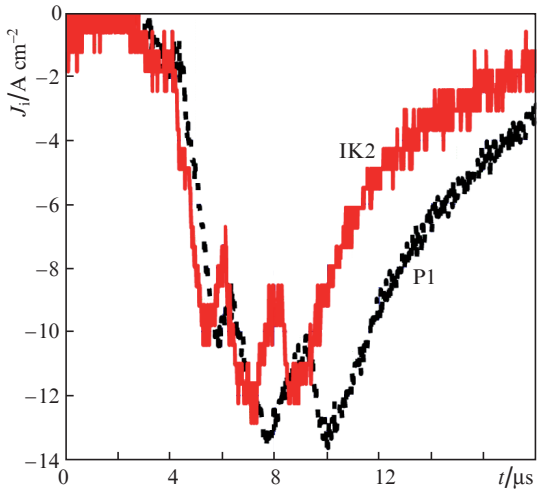

Figure 4. Dynamics of the flux density of ions J_i in the LP in the absence of magnetic field from the Langmuir probes IK2 and P1, located at distances $R_p = 59$ and 62 cm from the target at angles $\theta = 20°$ and 19° to the target normal, respectively.

of field expulsion R_b will amount to ~45 cm with the corresponding main criterion of the problem $\varepsilon_b = R_L/R_b \approx 0.27 < \varepsilon_b^* \approx 0.5$ (Table 1). This is obviously sufficient for intense interaction of the LP with the magnetic field and its deceleration at distances of $R_b \approx 45$ cm, which is confirmed by the summary data obtained from electric and magnetic probes on plasma deceleration and expulsion of the field at a distance of $R_p \approx 49$ cm (Fig. 5).

Table 1. Main parameters of a series of Super-Jet experiments at the KI-1 facility.

Regime	B_0/G	R_b/cm	R_L/cm	$\varepsilon_b = R_L/R_b$	Jet formation
1	150	73	26	0.36	no
2	200	60	19.5	0.33	?
3	300	45	12	0.27	yes

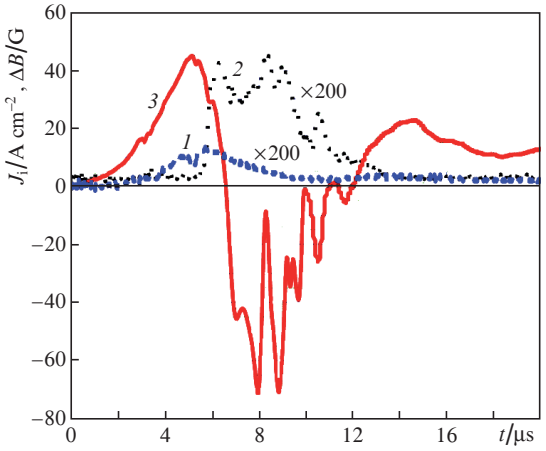

Figure 5. Data of the main set of Langmuir probes IK2 [(*1*) without a magnetic field, (*2*) at $B_0 = 300$ G] and a magnetic probe RM2H [(*3*), the main *z*-component] placed at a distance $R_p \approx 49$ cm from the target at an angle $\theta \approx 13°$ normal to the target.

3. Transverse jet formation and basic probe data on its internal structure and the dynamics of plasma and magnetic fields.

Figures 6 and 7 present experimental data on the formation of the jet and the three-dimensional structure of the initial diamagnetic cavity of the LP. Figure 8 shows additional data on the configuration and dynamics of the LP at the later stage of expansion obtained using the EOC at $B_0 = 300$ G (Figs 8a and 8b) and smaller fields 100, 150 and 200 G (Figs 8c–8e) (see Table 1). The most obvious signs of jet formation across the field were obtained in regime 3, as one would expect from the analysis of the fulfilment of the model experiment conditions in Section 2.

Basing on the comparison of the photographs shown in Figs 8a and 8d, one can assume that even at $B_0 = 200$ G the jet is formed at the time instant corresponding to the one expected from magnetohydrodynamic (MHD) scaling. Indeed, if the structures in Figs 8a and 8d are formed under similar MHD conditions, then they must have close dimensionless times $T = t/t^*$, where $t^* = R_b/V_0$ is the characteristic time of the MHD process, equal to 3.2 μs for the field of 300 G and 4.3 μs for $B_0 = 200$ G. Therefore, the dimensionless

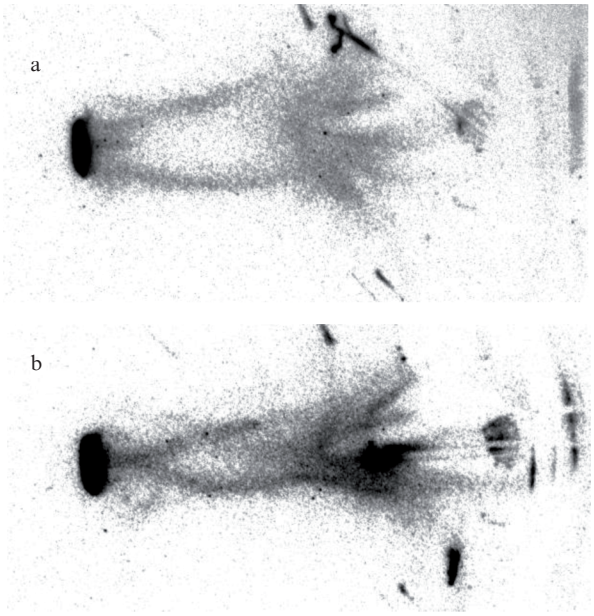

Figure 6. Structure and dynamics of the LP jets in the transverse magnetic field $B_0 = 300$ G at the instants of time t = (a) 8.5 and (b) 9 μs. The dark spot on the left has a vertical size of 11.5 cm. The light spot inside of plasma approximately corresponds to the size of the diamagnetic cavity that has detached from the target and begins to collapse.

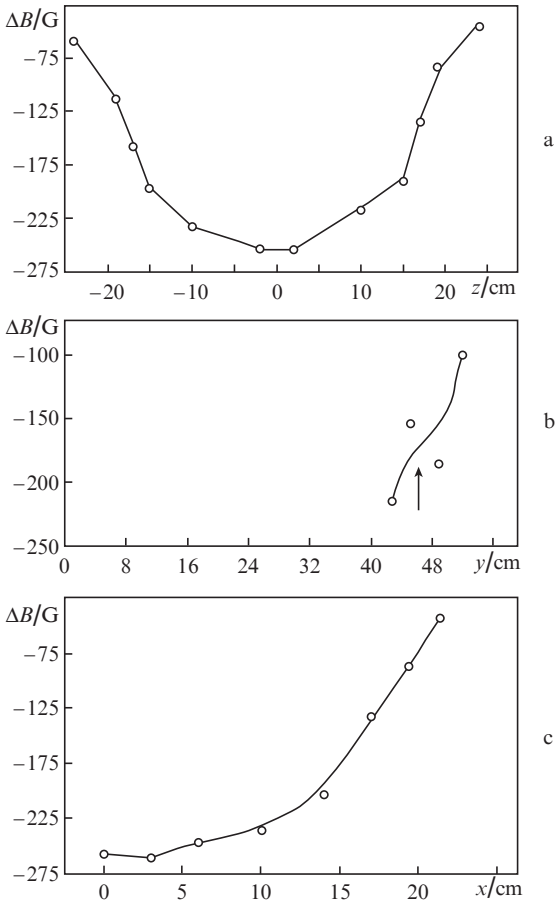

Figure 7. Profiles of the expulsion of the main component of the field $\boldsymbol{B}_z$ along the directions (a) z, (b) y and (c) x in the diamagnetic LP cavity at the moment of time $t = 6$ μs, when the expulsion of the magnetic field $B_0 = 300$ G is maximal. The arrow indicates the boundary of the cavity.

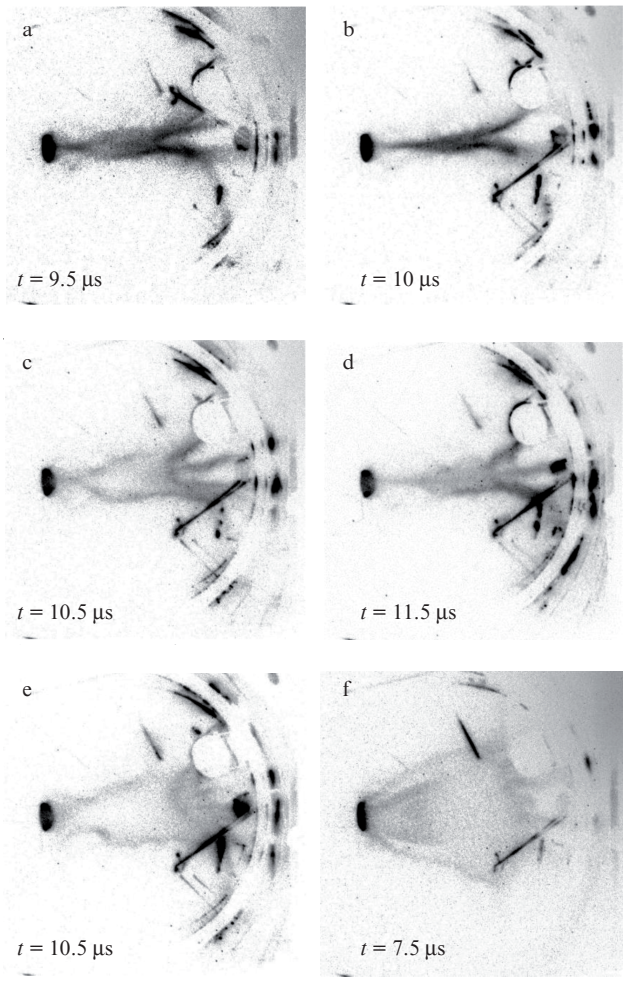

Figure 8. Configuration and dynamics of the LP at the late stage of expansion with a field of B_0 = (a, b) 300, (c, d) 200, (e) 100 and (f) 150 G at different moments of time.

moments of time are close and amount to ~3 and ~2.7 for these jet-like structures in Fig. 8.

Figures 9 and 10 show new data on the relationship between the structure and dynamics of plasma and magnetic fields at the late stage of the collapse of a diamagnetic cavity in such jets. While in the absence of a field (Fig. 9a) the dynamics of the ion flux J_i (from the IK2 probe) represents an ordinary solitary pulse, in the case of $B_0 = 300$ G (Fig. 9b) and 200 G (Fig. 10) the second pulse appears. This is a well reproduced (in shape, amplitude, and moment of appearance) pulse propagating 'inward' toward the plasma axis, with a certain constant velocity depending on the field B_0. The analysis shows that according to the locations and dynamics of the fronts, these additional pulses correspond to the movement of the inner light region of the jets (Figs 6 and 8). Note that in Ref. [10] a similar effect was registered only using the EOC.

Thus, the interrelation of concentration maxima with disturbances on the trailing edge of the cavity (indicated in Figs 9b and 9c by up and down arrows), which was first recorded in the Super-Jet experiment, is a completely new experimental data needed to construct complete physical models of such jets. In this case, the appearance of Hall effect is possible, since the velocity of magnetic-field fronts inward propagation is very likely proportional to B_0 (like the Alfvén

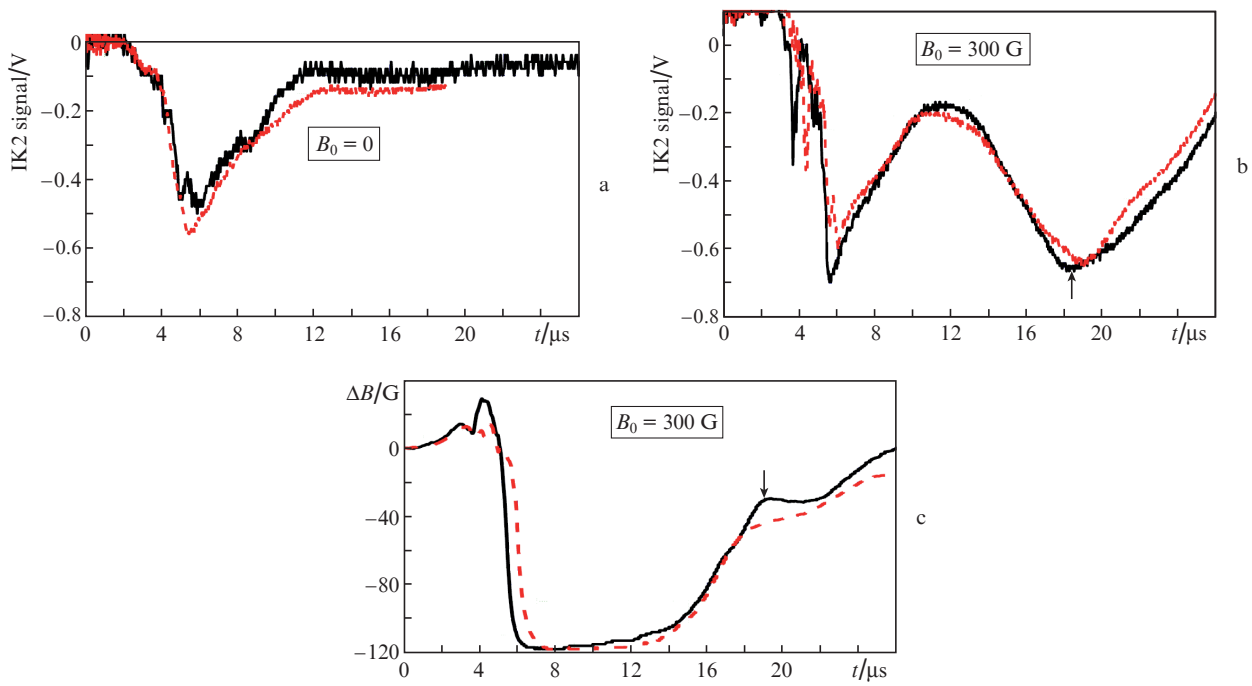

Figure 9. (a, b) Plasma and (c) magnetic field dynamics according to the data from the Langmuir IK2 probe and RM2H magnetic probe at the point ($x \approx 6$ cm, $y \approx 62$ cm) at the distance $R_p \approx 63$ cm from the target (at the angle $\theta \approx 7°$ to the target normal). Each figure shows two experimental implementations obtained under the same conditions.

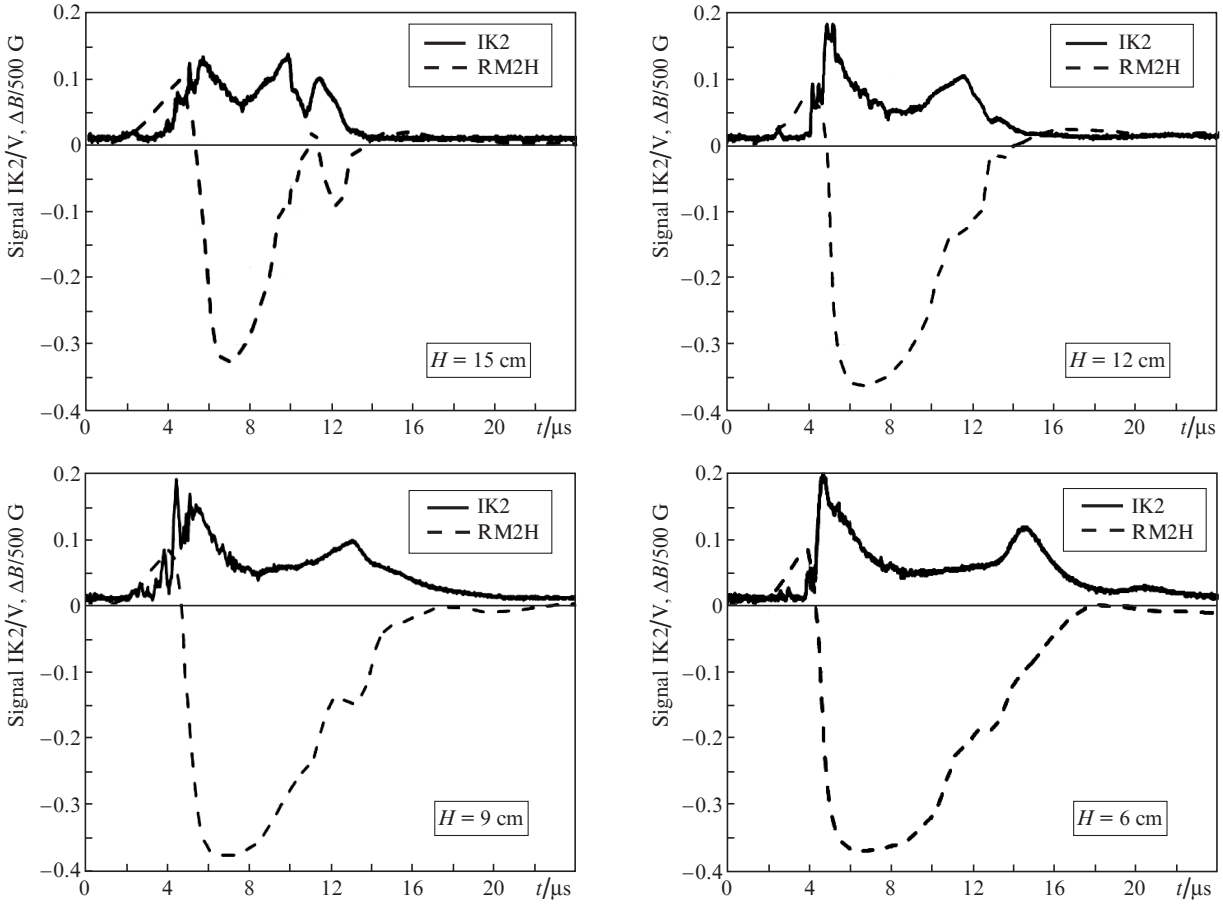

Figure 10. Dynamics of plasma (IK2 signal) and magnetic field (RM2H signal) in a magnetic field with $B_0 = 200$ G at different heights H (measured along the x axis) at $y = 47$ cm.

velocity itself, which is characteristic [26–28] of many processes in Hall magnetohydrodynamics).

A preliminary conclusion from the comparison of the obtained data demonstrates, first of all, that a new type of model experiments with high-energy LP is promising for the implementation of small values of the ion magnetisation criterion ($\varepsilon_b \leqslant 0.3$) on large spatial scales (1 m or larger) using large plasma setups (with the field up to 1 kG) with high-power laser systems ($Q \geqslant 1-2$ kJ). In this case, the Hall effect may manifest itself as a joint motion of the plasma and the magnetic field into the jet, towards its axis.

4. Conclusions

Analysis of the data obtained in the Super-Jet experiment with LP having high effective energy ($E_{e0} \approx 250$ J) at moderate magnetic fields B_0 (up to 300 G) on the KI-1 facility showed that a collimated large-size jet (up to ~70 cm along and ~30 cm across the initial velocity $\boldsymbol{V}_0$ of the LP, respectively) was for the first time formed and investigated in a transverse magnetic field $\boldsymbol{B}_0 \perp \boldsymbol{V}_0$. Using a system of electric and magnetic probes, as well as EOC-aided imaging, we found that when a flat polyethylene target was irradiated with a CO_2 laser focused into a spot ~2.5 cm in diameter (in the absence of magnetic field, a quasispherical plasma expansion occurs under these conditions [21–23] in a large solid angle $\Omega \geqslant 1$ sr), a plasma bunch at the initial stage (at $t \approx 6-7$ μs) of interaction with a field having a strength of 300 G produces a magnetic cavity, the size of which reaches the calculated size normal to the target $R_b = (3E_0/B_0^2)^{1/3} \approx 45$ cm for the effective energy $E_{e0} = 250$ J, the real kinetic energy of the LP being $E_0 = 50$ J. In this case, local development of the Hall-type flute instability is observed [19, 20]. Upon further expansion of the decelerated (velocity of expansion $\sim V_0/2$) LP bunch across the field with a strength of 300 G, a jet longer than half a meter is formed from it, inside which the magnetic plasma cavity collapses abnormally quickly towards the horizontal axis of the jet. In this case, the overall geometry of the expansion of the LP in the form of a jet has an essentially three-dimensional character, since a significant part of the plasma expands along the direction of the magnetic field.

Thus, considering the self-consistent action of the new effects revealed in the course of this experiment, as well as other effects investigated theoretically [29] and experimentally [10], it becomes possible to construct a complete model of such transverse jets. In particular, it is necessary to establish the main physical process that ensures the conservation of the total initial momentum of the plasma. We point out that the formation of jets requires a free space of sufficient size, at least $2R_b$.

We also note that in one of the most powerful and unique laser systems in Russia, the Iskra-5 with a magnetic field in a vacuum chamber of 1000 G, a laser pulse energy of $Q \approx 500$ J and duration of 1 ns (focused into a 3-mm spot), a jet-like structure transverse to the field with a length of up to ~20 cm and a diameter of ~6 cm was also recorded using the EOC [8]. However, it turned out to be very similar to the initial narrow jet of LP ($\Omega \ll 1$ sr) observed without the magnetic field. In the absence of probe measurements, it is possible to ascertain only a certain correspondence of the data on the transverse luminescence structure obtained at the Iskra-5 setup with those presented in this work, namely, the maxima at the edges of the jet are similar.

Acknowledgements. The work was carried out within the framework of Programme No. II.10.1.4 (0307-2017-0015) of the Fundamental Research of ILP SB RAS and Project 22 of the Programme 'Extreme Laser Radiation: Physics and Fundamental Applications' of the Presidium of the Russian Academy of Sciences.

References

1. Gribkov V.A., Krokhin O.N., Nikulin V.Ya. et al. *Sov. J. Quantum Electron.*, **5**, 530 (1975) [*Kvantovaya Elektron.*, **2**, 975 (1975)].
2. Zhong J., Yuan X., Han B., et al. *High Power Laser Science and Engineering*, **6**, e48 (2018).
3. Mostovich A.N., Ripin B.H., Stamper J.A. *Phys. Rev. Lett.*, **62**, 2837 (1989).
4. Peyser T.A., Manka C.K., Ripin B.H., Ganguli G. *Phys. Fluids B*, **4**, 2448 (1992).
5. Kasperczuk A., Pisarzyc T., Zakharov Yu.P. *Laser Part. Beams*, **17**, 537 (1999).
6. Zakharov Yu.P., Eremin A.V., Orishich A.M., et al. *Adv. Space Res.*, **29**, 1351 (2002).
7. Mishin E.V. *J. Geophys. Res. A*, **118**, 5782 (2013).
8. Bessarab A.V., Bondarenko G.A., Garanin S.G., et al. *Plasma Phys. Rep.*, **37**, 802 (2011) [*Fiz. Plazmy*, **37**, 858 (2011)].
9. Plechaty C., Presura R., Esaulov A.A. *Phys. Rev. Lett.*, **111**, 185002 (2013).
10. Behera N., Singh R.K., Chaudhari V., Kumar A. *Phys. Plasmas*, **24**, 033511 (2017).
11. Li C., Tzeferacos P., Lamb D., Gregori G., et al. *Nature Communications*, ncomms13081 (2016).
12. Albertazzi B., Giardi A., Nakatsutsumi M., et al. *Science*, **346**, 325 (2014).
13. Manuel M., Kuranz C.C., Rasmus A.M., et al. *High Energy Density Phys.*, **17**, 52 (2015).
14. Higginson D.P., Revet G., Khiar B., et al. *High Energy Density Phys.*, **23**, 48 (2017).
15. Krauz V.I., Myalton V.V., Vinogradov V.P., Velikhov E.P., et al. *J. Phys. Conf. Ser.*, **907**, 012026 (2017).
16. Zakharov Yu.P., Ponomarenko A.G., Terekhin V.A., et al. *Proc. VIII Int. Symp. on Modern Problems of Laser Physics (MPLP-2018)*(Novosibirsk) pp. 228, 229.
17. Giardi A., Vinci T., Fuchs J., et al. *Phys. Rev. Lett.*, **110**, 025002 (2013).
18. Raizer Yu.P. *Prikl. Mekh. Tekh. Fiz.*, (6), 19 (1963).
19. Zakharov Yu.P., Orishich A.M., Ponomarenko A.G. et al. *Sov. J. Plasma Phys.*, **12**, 674 (1986) [*Fiz. Plazmy*, **12**, 1170 (1986)].
20. Zakharov Yu.P., Antonov V.M., Boyarintsev E.L. et al. *Plasma Phys. Rep.*, **32** (3), 183 (2006) [*Fiz. Plazmy*, **32**, 207 (2006)].
21. Zakharov Yu.P., Ponomarenko A.G., Tishchenko V.N. et al. *Quantum Electron.*, **46**, 399 (2016) [*Kvantovaya Elektron.*, **46**, 399 (2016).
22. Akhsakhalyan A.D., Talonov S.V., Luchin V.I. et al. *Zh. Tekh. Fiz.*, **58**, 1885 (1988).
23. Anisimov S.I., Luk'yanchuk B.S. *Phys. Usp.*, **45** (3), 293 (2002) [*Usp. Fiz. Nauk*, **172**, 301 (2002)].
24. Mora P. *Phys. Fluids*, **25**, 1051 (1982).
25. Zakharov Yu.P., in *Entsiklopediya nizkotemperaturnoi plazmy* (Encyclopaedia of Low-Temperature Plasma. Ed. by V.E. Fortov) (Moscow: Nauka, 2000) Vol. II, pp. 463, 488.
26. Fruchtman A. *Phys. Fluids B*, **3**, 1908 (1991).
27. Swanekanp S.B., Grossman J.M., Fruchtman A., et al. *Phys. Plasmas*, **3**, 3556 (1996).
28. Hamlin N.D., Seyler C.E., Khiar B. *Phys. Plasmas*, **25**, 042906 (2018).
29. Moritaka T., Kuramitsu Y., Liu Yao-Li, Chen S.-H. *Phys. Plasmas*, **23**, 032110 (2016).